PHILOSOPHICAL TRANSACTIONS OF THE ROYAL SOCIETY A MATHEMATICAL, PHYSICAL & ENGINEERING SCIENCES

Kinetics of Structural Relaxations in a Two-Dimensional Model Atomic Glass III

D. Deng, A. S. Argon and S. Yip

Phil. Trans. R. Soc. Lond. A 1989 **329**, 595-612
doi: 10.1098/rsta.1989.0091

Phil Trans. R. Soc. Lond. A **329**, 595–612 (1989) [595]
Printed in Great Britain

KINETICS OF STRUCTURAL RELAXATIONS IN A TWO-DIMENSIONAL MODEL ATOMIC GLASS III

BY D. DENG†, A. S. ARGON AND S. YIP
Massachusetts Institute of Technology, Cambridge, Massachusetts 02139, *U.S.A.*

(*Communicated by M. F. Ashby, F.R.S. – Received 22 September* 1988)

CONTENTS

PAGE

1. INTRODUCTION 595
2. DETAILS OF THE SIMULATION 596
   2.1. The simulation cell 596
   2.2. Choice of boundary mass in the simulation 597
3. RESULTS 598
   3.1. Time-dependent changes in structural properties 598
   3.2. The kinetics of structural relaxation 600
   3.3. Inhomogeneities and clustering of atomic motions 606
4. DISCUSSION 609

APPENDIX 1. BOUNDARY MASSES 610

REFERENCES 612

The kinetics of structural relaxation in a two-dimensional model atomic glass quenched infinitely rapidly from the melt to 0.55 of the glass transition temperature was simulated by the molecular dynamics methods to study the chronological ordering of the atomic kinematics associated with such relaxations. Over the very short periods of ageing (*ca.* 200 atomic fluctuations) accessible to the molecular dynamics (MD) method, a Williams–Watts form of relaxation with a fractional exponent of 0.5 was found to hold for excess enthalpy, free volume and site distortion parameter. The distribution of free energy barriers associated with the relaxation that resulted from the analysis could be scaled up to describe processes occurring on macroscopic timescales, and agrees well with experimental results in Cu_xZr_{1-x} glasses. Results on the clustering of relaxations and other topological features of the relaxation process are also reported.

1. INTRODUCTION

The atomic details of structural alterations of amorphous solids during ageing below their glass transition temperatures and the consequences of this on subsequent inelastic behaviour has been of considerable interest. Simulation of such complex atomic processes by computer molecular dynamics (MD) has been very informative in the past. Among many such simulations

† On leave from the Institute for Precious Metals, Kunming, Yunnan Province, People's Republic of China.

those of Takeuchi and co-workers (Takeuchi *et al.* 1983; Kobayashi & Takeuchi 1984) on two component atomic glasses of the Cu_xZr_{1-x} type, carried out in three dimensions have resulted in considerable insight into structural relaxations. Despite this, however, both the kinematics and the kinetics of such relaxations remain inadequately understood. We have carried out a detailed MD simulation using the same truncated Cu and Zr pair potentials used by Kobayashi *et al.* (1980), but in two dimensions for the specific purpose of a more thorough understanding of the atomic mechanisms of plastic flow in simple atomic amorphous media. In three related papers, we have reported results of a simulation: on the melting and glass transition process in a two-dimensional idealized material (Deng *et al.* 1989*a*, referred to here as part I); on the topological features of structural relaxations in such a medium, both in subcooled melts and in solids below their T_g (Deng *et al.* 1989*b*, referred to here as part II); and on the details of large strain plastic shear (Deng *et al.* 1989*c*, referred to here as part IV). Here, in this same series of studies, we report on the kinetics of structural relaxations below T_g in the same two-component amorphous medium modelled in two dimensions. We also give additional details of some of the topological features in the material, which is more prone to undergo structural relaxation than the average.

2. Details of the simulation

2.1. *The simulation cell*

The details of the MD simulation, the choice of the interatomic pair potential of interaction, its truncation, the two-dimensional simulation cell with its periodic boundary conditions, and the normalization of parameters were given in part I. Additional details on the intensive state parameters, such as atomic level stresses, moduli, enthalpy, site distortion and local free volume were given in part II, Together with many results on the topological details of structural relaxations. The results of the simulation we present here were the same rectangular cell containing 144 atoms of two types representing Cu and Zr, placed initially randomly, and melted and quenched, as described in part I. The simulations reported here were at a temperature of $T^* = 0.1$ $(= 0.4T_m^*)$ and under a constant external normalized pressure of $p^* = 1.0$. This temperature is well below the glass transition temperature of $T_g^* = 0.18$. The starting state of the material was one which had seen an essentially infinite quenching rate (path EF in figure 1 of part II) from the melting temperature of 0.25, i.e. the starting material had a fictive temperature equal to the equilibrium melting temperature. Many topological details of structural relaxation of this quenched glass were reported in part II. The magnitude of the so-called boundary mass used in the present simulation to maintain the external pressure constant was 4. The concept of a boundary mass associated with the volume of the simulation cell as an extra degree of freedom to maintain the external pressure constant was introduced by Andersen (1980). It has been widely used in MD simulations where only equilibrium structural properties are of interest, and the kinetics of reaching the equilibrium is not. In this simulation, however, where the kinetics of structural relaxation were of equal interest as the topological details of the atom exchanges, the proper choice of the boundary mass was an important consideration.

2.2. *Choice of boundary mass in the simulation*

In the method of Andersen (1980), simulation under constant external pressure is accomplished by the introduction of a new dynamic variable Q, which represents the changes in the overall volume of the simulation cell. Then, the equations of motion of all n atoms in the system and the cell volume are derivable from a modified lagrangian L given by

$$L(\rho_i, \dot{\rho}_i, Q, \dot{Q}) = \tfrac{1}{2}mQ^{\frac{2}{3}} \sum_{i=1}^{n} \dot{\rho}_i \cdot \dot{\rho}_i - \frac{1}{2} \sum_{\substack{j=1 \\ j \neq i}}^{n} \phi(Q^{\frac{1}{3}}\rho_{ij}) + \tfrac{1}{2}M\dot{Q}^2 - \alpha Q, \tag{1}$$

where $\rho_i (r_i/Q^{\frac{1}{3}})$ are dimensionless position coordinates of the n atoms, $\dot{\rho}_i$ their velocities, ρ_{ij} the dimensionless relative separations of atoms i and j, ϕ the pair potential, m the mass of an atom, Q the coordinate representing the volume viewed as a one-dimensional entity, such as the length of a cylinder capped by a piston, α a constant to be interpreted as the external force resulting from the external pressure acting across the boundaries of the simulation cell in a work conjugate sense with the volume coordinate Q, and finally M, the so-called boundary mass (all symbols not defined here are as in part I, where a full list can be found). In (1) the first two terms on the right-hand side represent the normal lagrangian of the system of n particles if Q is interpreted as the volume. The third and fourth terms relate to the lagrangian of the total volume of the cell in the interpretation of Q as the added dynamic variable representing the volume. The generalized velocities and momenta that result from this scaled lagrangian, and how they can be related to the real system, has been discussed in detail by Andersen (1980) and need not be repeated here. It should suffice, however, to observe that the introduction into the system of a pseudo-coordinate to represent the volume, and a pseudo-mass associated with it, permits maintaining the external pressure constant by permitting the volume to change as necessary. Clearly, however, this introduces into the simulation system a new normal mode and a new momentum with an added normal mode frequency that can interact with the other physically meaningful modes of atoms, and may result in unwanted resonances. It can be shown, and is also readily clear, that the introduction of this pseudo-coordinate does not affect the equilibrium properties of the system and its topological features in equilibrium. It will, however, influence the kinetics of reaching equilibrium, and the topological features of non-equilibrium states that are of interest in the simulation. Andersen has proposed that unwanted artefacts in the kinetics can be reduced if the boundary mass M is chosen so that the period of the fluctuation of Q in the scaled system is approximately equal to $Q^{\frac{1}{3}}$ divided by the speed of sound in the simulation medium, when Q is equated to the volume. For a simulation cell containing 144 atoms this rule results in a boundary mass $M = 3.65m$ of individual atom masses. We have taken 4 as the nearest integer value to be used in the simulation. In addition, however, we have tried simulations of structural relaxations with boundary masses of 400 and 0.04 to determine the sensitivity of the results on this choice. Thus, as presented in Appendix 1, whereas a choice of $400m$ for the boundary mass produced overdamped conditions, very markedly slowing down the structural relaxation, a choice of $0.04m$ produced erratic results.

3. Results

3.1. *Time-dependent changes in structural properties*

The time-dependent changes in several ensemble average intensive structural properties for a period of 200 fluctuations (4000 time steps) are shown in figure 1*a–g*. Here, the period of an atomic fluctuation is taken as 5.4×10^{13} s (see part I). The figures show both the level of fluctuations in overall average properties, as well as their monotonic changes over this period, first, for the entire ensemble of 144 atoms, but also for the subensembles of Zr and Cu atoms, as marked. Among these, figure 1*a* shows the changes in the average Voronoi polygon volume per atom (r_0 times area per atom). Clearly, the regular fluctuations due to the boundary mass are apparent, not only in the fluctuations of the volume, but to some extent in all other properties, as can be seen by inspection of figure 1*b–g*. Figure 1*b*, *c*, for example, show the corresponding changes in the ensemble average values of the enthalpy and site distortion parameter (for definitions of these intensive parameters describing structural properties of the glassy state, refer to part II), while figure 1*d–g* give the related changes in the atomic site pressure, maximum shear stress (in the plane, regardless of orientation), the *xy* shear stress, and the atomic site bulk modulus, all averaged over the entire ensemble as well as over only the Zr atoms and the Cu atoms, as indicated in the figures. The averaging has been done for every fluctuation, i.e. after every 20 time steps without any smoothing. Clearly, as stated above, the major and regular fluctuations with a period of about 18 atomic fluctuations is due to the border mass and must be ignored. When these are discounted, there is a clear trend of decrease in the volume, enthalpy and site distortion. Large local fluctuations, however, remain, particularly in the atomic level stresses and local bulk moduli. Additionally, it is evident that the atomic site pressures, maximum shear stresses, and bulk moduli for the Zr atoms, are much larger than the average, while the reverse is true for the Cu atoms. As already noted in part II, this is a direct result of the stiffer environment of the Zr atom than that of the Cu atom. The effect of this on the enthalpy fluctuations is in the reverse order, where, as must be the case, more energy is stored, on the average, in the more compliant surroundings of the Cu atoms. Furthermore, it can also be observed that in the regular oscillations of the boundary mass, the fluctuations of the Voronoi volume and the atomic pressure are out of phase, i.e. as the atomic site pressure increases, the local volume decreases, and the atomic site bulk modulus increases. This direct response of the local site properties under the action of the boundary mass, however, does affect the kinetics of structural relaxation by speeding it up to some extent (see Appendix 1). We note from figure 1*a–g* that there are substantial reductions in excess properties (over and above those of an ordered hexagonal crystal) in enthalpy, local volume per atom (Voronoi volume), and site distortion over the total relaxation span of 200 fluctuations. There is a corresponding increase in the local bulk moduli from 17 to about 18 (in units of dimensionless pressure) or by an amount of 6%. In comparison, there are no important relaxations in the atomic level pressures and maximum shear stresses. As the changes in enthalpy must come from the reduction in root mean square (r.m.s.) elastic strain energies, however, it must be concluded that the observed changes come about primarily from the increases in bulk modulus and a corresponding increase in atomic level shear moduli. Although all ensemble average properties fluctuate considerably, the ratio of the average fluctuation amplitude to the current average level of the property show large differences between different properties. These ratios are listed in table 1 and indicate that, initially, the ratios are largest

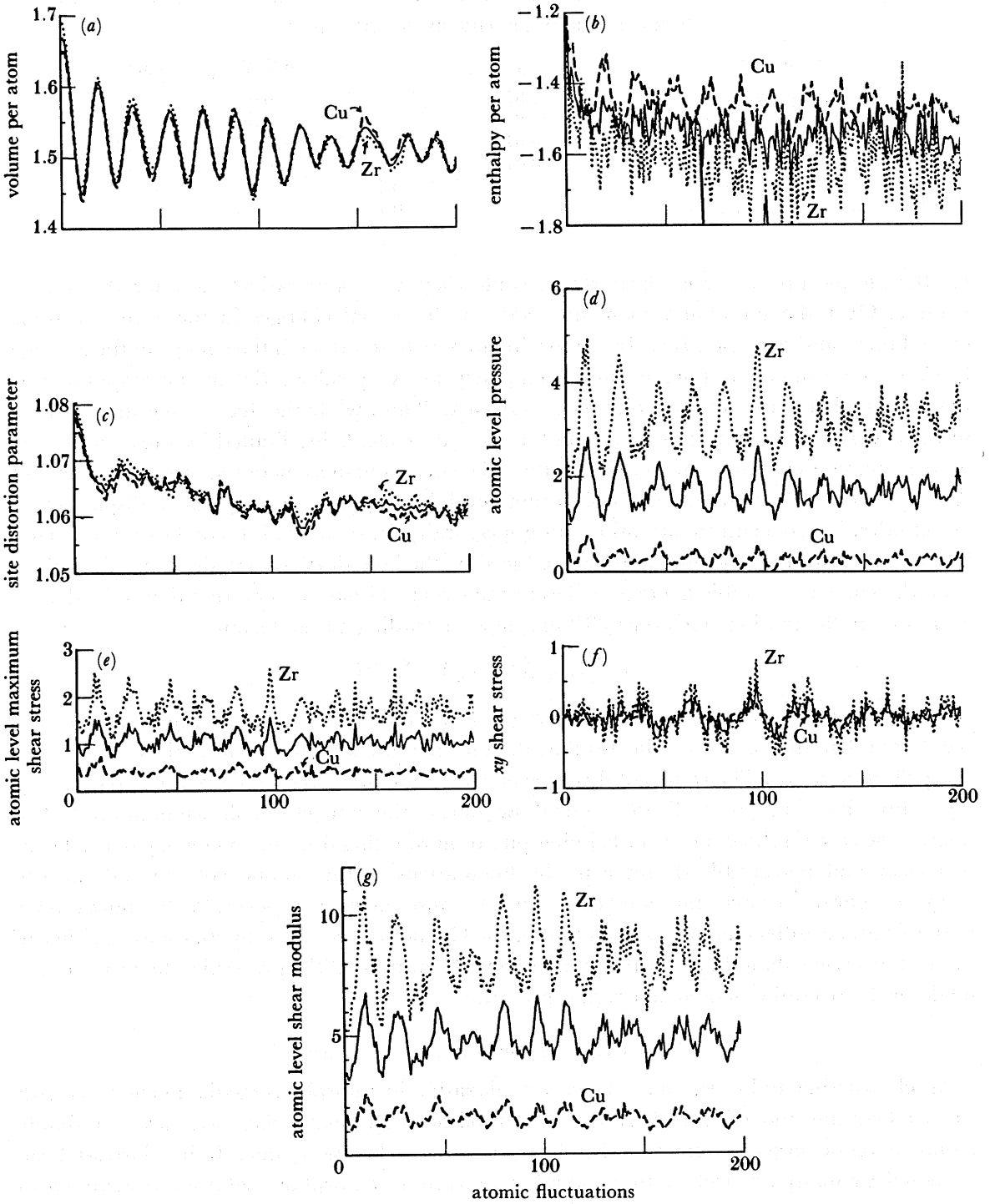

FIGURE 1. Time dependent changes in ensemble averages over 200 fluctuations (= 4000 time steps): (*a*) volume per atom; (*b*) enthalpy; (*c*) site distortion parameter; (*d*) atomic level pressure; (*e*) atomic level maximum shear stress; (*f*) *xy* shear stress; (*g*) atomic level shear modulus. Ensemble averages are given both for the entire population as well as for the Zr and Cu atoms separately.

PHILOSOPHICAL TRANSACTIONS OF THE ROYAL SOCIETY A MATHEMATICAL, PHYSICAL & ENGINEERING SCIENCES

Table 1. Ratios of fluctuation amplitudes to average levels in structural parameters over the simulation span

parameter	$(\Delta X/\bar{X})_{\text{initial}}$		$(\Delta X/\bar{X})_{\text{final}}$	change (%)
atomic pressure	1.07		0.6	44
atomix max. shear stress	0.8		0.5	38
atomic bulk modulus	0.57		0.45	21
atomic volume	0.07		0.03	57
enthalpy per atom		0.2		
distortion parameter		0.1		

for the atomic pressure and shear stress, while they are comparatively low for the atomic volume. Over the simulation span, however, the fractional changes in the atomic volume exceed those in the stresses. It is also interesting to note that although the change in the average levels of the atomic stresses are quite small, they are very substantial in the amplitudes of fluctuation. The source of these differences are clear. Thus, while the fluctuations and changes in the atomic volume are quite small on the absolute scale, being limited by the overall level of free volume that can be squeezed out, the stresses can fluctuate between large negative and large positive values about an equilibrium level in response to only small displacement amplitudes. To concentrate attention more specifically on the actual fluctuations, unaffected by the superimposed large fluctuations produced by the boundary masses, the r.m.s. deviations from the current ensemble average values in the structural parameters were determined after each atomic fluctuation (for every 20 time steps) according to the formula

$$X_{\text{rms}} = \langle (X(i) - \langle X(i) \rangle_t)^2 \rangle_t^{\frac{1}{2}}. \tag{2}$$

In (2) the brackets mean ensemble averages over either the entire population or over only the Zr and Cu atoms, and t indicates that the information is evaluated at a given time (after every 20 time steps). The results of this type of evaluation are given in figure 2*a–g*, paralleling the results given in figure 1. These results show some of the same effects shown in figure 1. The fluctuations do not show the overwhelming pulsation resulting from the boundary mass. There is a clear and perceptible decrease in the fluctuations in the atomic volume and the site distortion parameter over the simulation span. Because the average levels for the fluctuations of the Zr atoms differs markedly from that of the Cu atoms, the r.m.s. fluctuations in either of these atoms is less than that over the entire ensemble for most of the properties, by virtue of the mode of the overall ensemble averaging procedure.

3.2. *The kinetics of structural relaxation*

Much experimental research on structural relaxation in amorphous media, in common with stress relaxation and internal friction, has established that such relaxations are not simple mono-energetic processes characterizable by a single relaxation time. It has instead been proposed by many researchers that the relaxations in an amorphous solid are distributed in relaxation time, or in a somewhat more fundamental variant, that they are distributed in activation energy and frequency factor. From this point of view, which we have taken earlier (Deng & Argon 1986*a*, *b*), in a narrow range of observation the relaxation of any property can be characterized by a simple exponential, given by

$$\psi_i(t) = (X_i(t) - X_i(\infty))/(X_i(0) - X_i(\infty)) = \exp(-t/\tau_i), \tag{3}$$

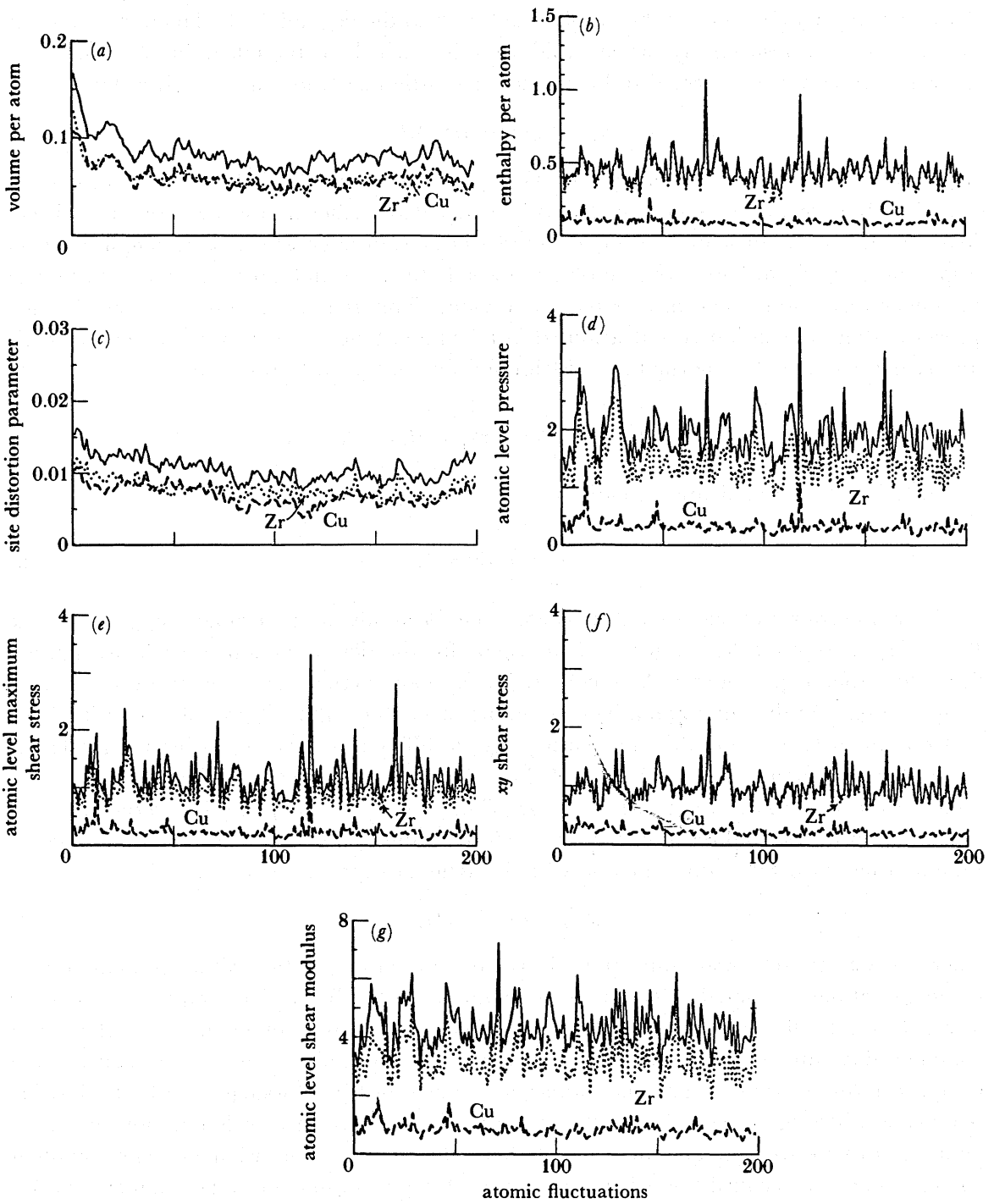

FIGURE 2. Time dependent changes in root mean square deviations from the ensemble mean values over 200 fluctuations: (*a*) volume per atom; (*b*) enthalpy; (*c*) site distortion parameter; (*d*) atomic level pressure; (*e*) atomic level maximum shear stress; (*f*) *xy* shear stress; (*g*) atomic level shear modulus.

where $\psi_i(t)$ is the level of the normalized property at time t of an element i and $X_i(t)$, $X_i(0)$ and $X_i(\infty)$ are the actual values of the property at time t, at the beginning of relaxation and at the end of relaxation respectively, when equilibrium is reached. As the relaxation is a thermally activated process, it is expected to have a characteristic relaxation time τ_i, given by:

$$\tau_i = \tau_{i0} \exp(\Delta H_i / kT), \tag{4}$$

where ΔH_i is an activation enthalpy over the key barrier holding back the local relaxation and $1/\tau_{i0}$ is a fundamental frequency factor. It is then stated further that if the observation is not in a narrow range, but spans over many decades in time, or alternatively is accomplished over a span in temperature, other relaxation processes, both easier and more difficult, with shorter or longer relaxation times also become observable. This requires a superposition of many processes that are continuously distributed in relaxation time τ, according to a characteristic and structure-dependent normalized distribution function $p(\tau)$, to result in

$$\psi(t) = \int_0^\infty p(\tau) \exp(-t/\tau)\, d\tau, \tag{5}$$

and obeying the normalization condition

$$\int_0^\infty p(\tau)\, d\tau = 1. \tag{6}$$

Many procedures of operational inversion have been advanced (Primak 1955; Novick & Berry 1972; Argon 1968; Argon & Kuo 1980) for the determination of such distribution functions from experimental data collected over long periods of time or over different temperatures. On the other hand, based on quite successful empirical procedures dating back to Kohlrausch (1863) more than a century ago, a different approach has been suggested to account for the non-exponential form of the long term relaxation behaviour of amorphous media. In this approach, recently revived by Williams & Watts (1970), it is observed that the relaxation in the normalized property can be fitted quite well over a relatively wide range of time to a modified relaxation function with a fractional exponent given as

$$\psi(t) = \exp(-t/\tau_w)^\beta, \tag{7}$$

where τ_w is a new relaxation time and β is usually in the range of 0.5. Although many recent investigators have adopted this form of presentation on the basis of its simplicity, and have asserted that it reflects a more complex non-arrhenian relaxation, others have searched for a common denominator between the physically more appealing, but operationally more complex, form given in (5) and the simpler form given in (7) (Shlesinger & Montroll 1984; Bendler & Shlesinger 1985). Thus, the stretched exponential form of Kohlrausch has been found consistent with a random walk of thermally activated diffusion of some impotent configurations to a central site, where, upon arrival, a measurable unit relaxation event takes place. The fractional exponent then arises from a distribution of free energy barriers in the preparatory diffusion process of the key impotent configurations to the central site where they trigger the unit relaxation process. To obtain the fractional power β in the exponent of the exponential, it has been necessary to assume special distributions of barrier energies with exponential tails. Operational procedures have been developed further to obtain distribution functions of barrier heights in the diffusion problems from experimental data directly (Lindsey & Patterson 1960).

PHILOSOPHICAL TRANSACTIONS OF THE ROYAL SOCIETY A MATHEMATICAL, PHYSICAL & ENGINEERING SCIENCES

We consider these two different points of view as alternative operational approaches to represent the same physical phenomenon, in which the relaxation process is distributed in relaxation time or in activation energy and frequency factor. Whether the actual unit relaxation process is a sudden transformation of a local configuration from more open to more compact in one thermal fluctuation, or is composed of a series of prior impotent diffusive steps approaching a central site without any observable effect, finally triggering the observable unit relaxation process upon arrival at this site is difficult to decide. The topological details of the simulation described in some detail in part II indicate that in reality, the processes may be a combination of both pictures, where the central unit process is noted to be the dissolution of five- and seven-sided polygon dipoles. Noting difficulties in relating the Williams–Watts relaxation function uniquely to distribution functions of energies in preparatory diffusive processes (Lindsey & Patterson 1980), or performing an operational inversion to calculate $p(\tau)$ from equations of the type given in (5), we will merely adopt the Williams–Watts function and obtain the best fit of the results of our simulation to it. We justify this less than complete analysis by noting that the simulation covers only a very small portion of real time extending over only 200 atomic fluctuations, making it virtually impossible to obtain any relaxation times that are comparable with experimental information.

The results of fitting the ensemble averages of the evolving structure parameters presented in figure 1*a–g* to the Williams–Watts function are given in figure 3*a–g*. In these figures, the overall ensemble averages are shown by the fluctuating form. The best fit to the Williams–Watts function is given by the smooth solid curve to determine the exponent β and time constant τ_w. Finally, the dotted curves, also shown on many of the plots, represent the best fit to the simple relaxation function with $\beta = 1$ (equation (3)). The resulting best fit constants for the Williams–Watts relaxation function are given in table 2. We note from here that the relaxation of atomic volume, enthalpy and site distortion are all characterizable with nearly the same function having a relaxation time τ_w in the vicinity of seven fluctuations (= 140 time steps) and an exponent of $\beta = 0.5$. The relaxation of the shear modulus obeys nearly the same form of the equation with, however, a relaxation time of more than twice the length. In comparison, the relaxation of atomic site pressures and maximum shear stress are much slower, as is apparent from figure 1, and is characterizable by a very much longer time constant of around 53 fluctuations (= 1060 time steps) and a considerably larger exponent of $\beta = 0.85$ coming close to the simple relaxation process of (3).

Examination of figure 3*a–g* show that all ensemble properties decrease from quenched-in initial excess values to lower values during the simulation span of 200 fluctuations. The decreases are more dramatic and substantial for volume per atom, site distortion parameter and enthalpy than they are for the individual stresses. The ensemble averages of atomic site shear moduli actually increase, as they should. The decrease in the atomic site pressure is 3%, while that in atomic site maximum shear stress is 5%. The related rise in the atomic site shear modulus is 5%, while the rise in the atomic site bulk modulus could be determined to be 6% from the information given in figure 1*g*. The corresponding decreases in the ensemble average enthalpy is 14%, that for the volume per atom is 10%, and for the site distortion parameter only 2%. As the ensemble average fractional change of enthalpy must be predominantly coming from the change in internal strain energy stored partly in shear strain energy and partly in bulk compression strain energy, we estimate the fractional enthalpy change from

$$\Delta h/h \approx \Delta \ln \left((p^2/2K) + (\tau_{\max}^2/2\mu) \right) \Omega, \tag{8}$$

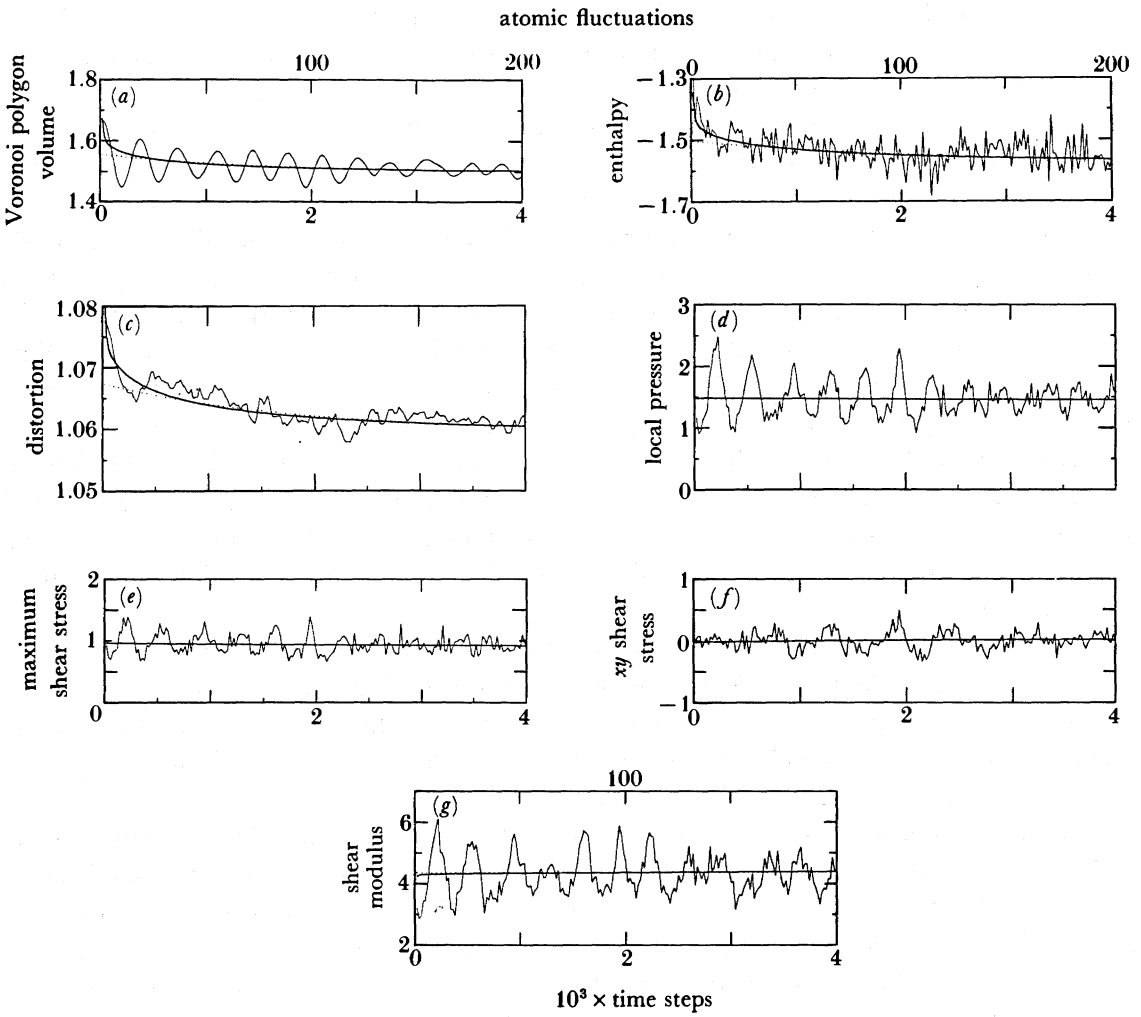

FIGURE 3. Best Williams–Watts function fits to the changes in ensemble averages for the same seven structure parameters given in figures 1 and 2.

where K is the bulk modulus and μ the shear modulus. Evaluation of (8) gives for $\Delta h/h$ exactly 14 % from the changes in pressure, maximum shear stress, bulk modulus, shear modulus and atomic volume. We consider this a good check on internal consistency in the simulation.

We note further, in passing, that the ratio of the ensemble average maximum shear stress to shear modulus is 0.21, while the corresponding ratio of average pressure to bulk modulus is 0.085. These are both somewhat higher than the ratios reported by Egami & Vitek (1983) for a three-dimensional amorphous medium. We attribute the difference to the two-dimensional nature of our material.

As the relaxation of most of the properties, except the atomic site stresses, can be characterized by a Williams–Watts function with a fractional exponent of 0.5 and a characteristic time constant $\tau_w = 7$ atomic fluctuations (= 240 time steps), it is possible to give a distribution function $p(\tau)$ of relaxation times of simple arrhenian processes on the basis of an analytical solution of the integral equation obtained by equating (5) and (7). This solution, obtained by Lindsay & Patterson (1980), gives

$$p(\tau) = \tfrac{1}{2}(\tau_w/\pi\tau)^{\frac{1}{2}}\tau_w^{-1}\exp(-\tau/4\tau_w). \tag{9}$$

For comparison with experimental results obtained by Deng & Argon (1986*a*), we convert this distribution into one of activation free energies ΔG^* by noting that

$$p(\Delta G^*)\,\mathrm{d}\Delta G^* = p(\tau)\,\mathrm{d}\tau = p(\Delta G^*/E_0)\,\mathrm{d}(\Delta G^*/E_0), \tag{10}$$

giving

$$p(\Delta G^*/E_0) = E_0 p(\Delta G^*) = E_0 p(\tau)\,\mathrm{d}\tau/\mathrm{d}\Delta G^*. \tag{11}$$

Upon introduction of the relations,

$$\tau/\tau_w = (\tau_G/\tau_w)\exp(\Delta G^*/kT), \tag{12a}$$

implying

$$\tau_G = (2\pi\nu_G)^{-1}, \tag{12b}$$

into equations (9)–(11) it is found that:

$$p\left(\frac{\Delta G^*}{E_0}\right) = \left(\frac{E_0}{kT}\right)\left(\frac{1}{2\sqrt{\pi}}\right)\left(\left(\frac{\tau_G}{\tau_w}\right)\exp\left(\frac{\Delta G^*}{E_0}\right)\left(\frac{E_0}{kT}\right)\right)^{\frac{1}{2}}\exp\left\{-\frac{1}{4}\left(\frac{\tau_G}{\tau_w}\right)\exp\left(\frac{\Delta G^*}{E_0}\right)\left(\frac{E_0}{kT}\right)\right\}, \tag{13}$$

where ν_G is a fundamental atomic cluster frequency related to the clusters which undergo structural relaxations. Noting that for the simulation $kT/E_0 = 0.1$, and taking ν_G as the atomic frequency, $\tau_G/\tau_w = 1/(14\pi)$ for $\tau_w = 7\tau_G$, as obtained from table 2, it is possible to evaluate the distribution function of (13) as a function of $\Delta G^*/E_0$. The result of this is given in figure 4.

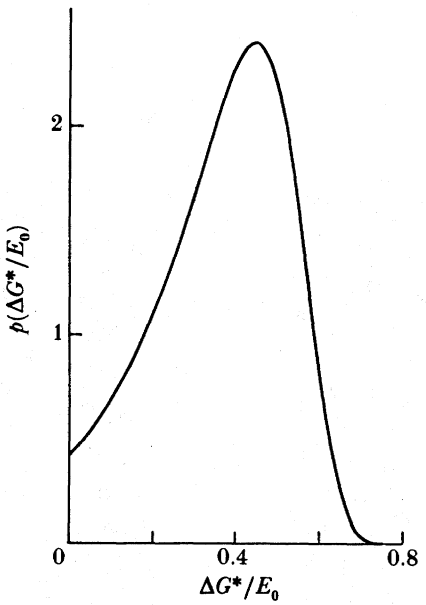

FIGURE 4. The free energy barrier distribution function for the structural relaxation, obtained from the Williams–Watts distribution function by an operational inversion.

TABLE 2. BEST FIT VALUES OF WILLIAMS–WATTS DISTRIBUTION PARAMETERS DETERMINED FROM RELAXATION SIMULATION

structure parameter	β	τ_w[a]	X_0	X_∞
atomic volume	0.55	130	1.668	1.504
enthalpy	0.5	140	−1.344	1.565
distortion parameter	0.55	150	1.082	1.060
atomic pressure	0.85	1060	1.486	1.454
atomic max. shear stress	0.85	1020	0.968	0.916
shear modulus	0.5	320	4.232	4.396

[a] In time steps (= 0.05 fluctuations).

While the shape of this figure compares favourably with that obtained by Deng & Argon (1986*b*) from internal friction measurements in a $Cu_{59}Zr_{41}$ alloy (their figure 8), the energy scale of the latter is a factor of 26.8 larger than the simulation results. This is not surprising, because the frequencies in the internal friction results were in the range of 0.25 Hz, while those in the simulation were no smaller than 10^{11} Hz.

3.3. *Inhomogeneities and clustering of atomic motions*

Figure 5*a–b*, show the total atom motions in two separate time periods of 10 fluctuations each (5*a* from 70–80; 5*b* from 100–110). The displacements, at a magnification of 10, are shown as bars emanating from the initial positions of the atoms at the beginning of the time period. The motions shown in these two frames are typical of many such frames that have been examined. In figure 5*a*, the motions are relatively random over most of the field, except in the central upper portion, where group-like displacements toward the left are evident. In figure 5*b*, on the other hand, very large group-like motions of atoms toward the left are visible in the entire right half of the simulation cell. Such large to and fro motions of blocks of atoms often reversed in the following 10 fluctuations. They are attributed to the resonances resulting from the boundary mass that show up clearly in the pulsations of the volume shown in figure 1*a* and were, therefore, largely ignored.

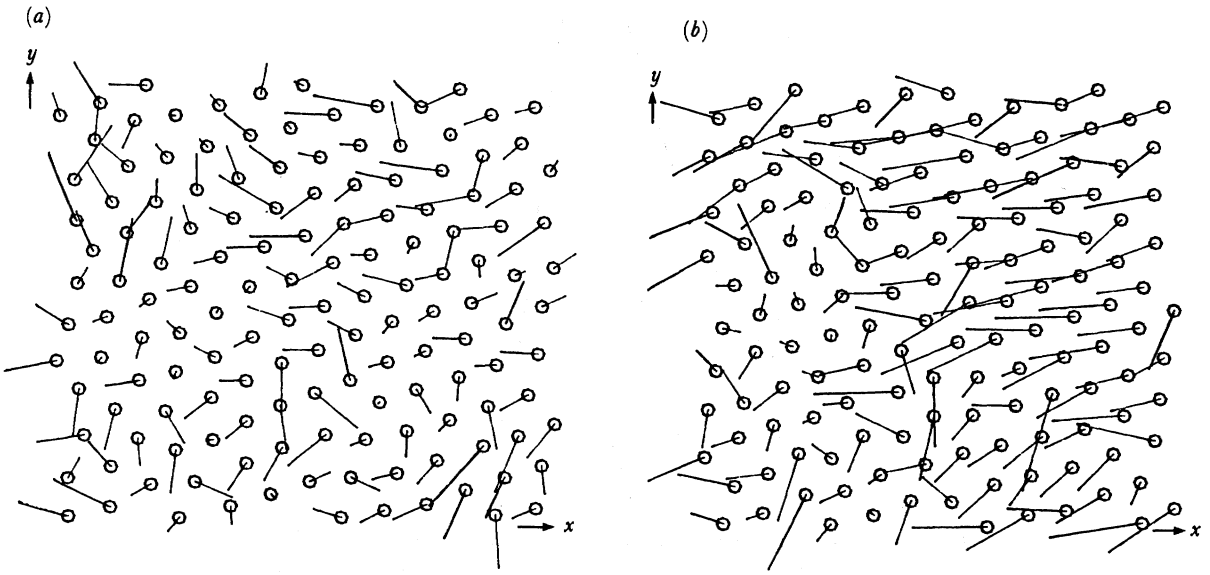

FIGURE 5. Two different states of incremental atom displacements during the simulation: (*a*) for the period between 70 and 80 fluctuations; (*b*) for the period between 100 and 110 fluctuations.

More importance was attached to the clustering of the atomic structure parameters, which were considered to be more genuine and were followed in some detail. Figure 6*a–c* show the clustering of enthalpy, volume per atom and site distortion parameter averaged over the entire simulation span of 200 fluctuations. The length of the solid horizontal bars reflect the relative magnitudes of the respective properties. All the atomic site properties encircled are larger than the ensemble average, except those in circles 3 and 5, which are smaller than the ensemble

average. The bars emanate from the centres of atoms. The atoms bearing numbers are the upper and lower 10 percentile of the population with largest and smallest properties. Clustering in atomic level pressure, maximum shear stress, *xy* shear stress and shear modulus, or bulk modulus, was less prominent. For these, the excess properties that were also large were, however, more uniformly mixed. These clusters in enthalpy, volume per atom and site distortion indicate that excess properties in the field have often long lifetimes and persist through even relatively long simulation spans. If they are to represent actual structural relaxations in real time, they must, of course, have lifetimes larger by orders of magnitude than the period of 200 fluctuations considered here. The evolution of properties in clusters and their random changes in size and shape was followed in more detail over smaller increments of the simulation span, but maps of these changes will not be presented here. From examination of these changes, however, the following important observations have been made.

1. Prominent clustering occurs only in excess enthalpy, volume per atom (free volume) and site distortion. These are also the properties that, as in figures 1 and 2, show the more prominent relaxation effects.

2. Clustering of atomic level stress is slight. The largest clusters of atoms with excess pressure or excess maximum shear stress were only 2–3 atoms across. Generally, it was found that atoms under large stress of all types, i.e. pressure, or maximum shear stress, were the Zr atoms, while those under the lowest pressure or shear stress were the Cu atoms. As these were initially randomly spaced, and because the simulation time spans were too short to produce much chemical short-range ordering, the lack of clustering is not surprising. As already noted, the clustering correlates with more prominent relaxation strength. Somewhat similar observations were also made by Maeda & Takeuchi (1982) in their study of radial correlation functions of the atomistic structure parameters, but they did not give a cause.

3. Comparison of the clustering in figure 6*a–c* shows that the clusters with high excess enthalpy tend to overlap with clusters having high excesses of free volume and those showing excesses of site distortion. Parenthetically, it must be observed that clustering of excess enthalpy requires clustering of a combination of dilatational and shear strain energy, which does not require clustering of either pressure or maximum shear stress.

4. Relief of site distortion in clusters of this property resulted in clustering of shear strains of random sign, which showed spatial correlation with the clusters of site distortion. A similar correlation was found between the relief of excess free volume and volumetric compaction.

5. Some spatial correlation was found between local shear-strain production during relaxation and increments in positive dilatation. Such dilatancy is known to be a prominent effect during imposed shear strains. The importance of this effect is more clearly demonstrated in the companion study (part IV) of simulations of plastic-shear deformation (Deng *et al.* 1989*c*).

6. It was found generally that regions with excesses of free volume coincided with regions of reduced bulk modulus or shear modulus or both, while the opposite was true for regions of deficiency of free volume. This is considered to be an important source of distribution in frequency factor found by Deng & Argon (1986*b*) in internal friction experiments in $Cu_{59}Zr_{41}$ glasses.

7. Comparison of the clustering of site distortion with distributions of Voronoi polygons with sides other than six, reported in part II, showed a necessary correlation between large distortions and non-hexagonal polygons.

PHILOSOPHICAL TRANSACTIONS OF THE ROYAL SOCIETY A MATHEMATICAL, PHYSICAL & ENGINEERING SCIENCES

In summary, we note that three types of clusters were observed: an excess volume cluster (free volume), called an n cluster by Egami & Vitek (1983), has a lower local pressure and a lower local modulus; a cluster of deficiency of volume, called a p cluster by Egami & Vitek, which possesses a higher local pressure and a higher local modulus; and finally, a site distortion cluster, which possesses a higher level of maximum shear stress and also an excess of volume. Only the first and third type of cluster undergo important evolution during structural relaxation, while the first contracts the third undergoes a combined shear and dilatation. The changes in the p type cluster are far less consequential or apparent.

The evolution of properties in five clusters were studied in more detail as a function of time during the simulation. These, marked 1–5 in figure 6*a*, *c*, each contain roughly equal numbers of Zr and Cu atoms. Cluster 1 possessed a substantial excess of volume per atom in the initial state. Clusters 2 and 4 possessed a large excess in site distortion, while clusters 3 and 5 had quite low levels of excess volume per atom. The changes in volume per atom, enthalpy, site

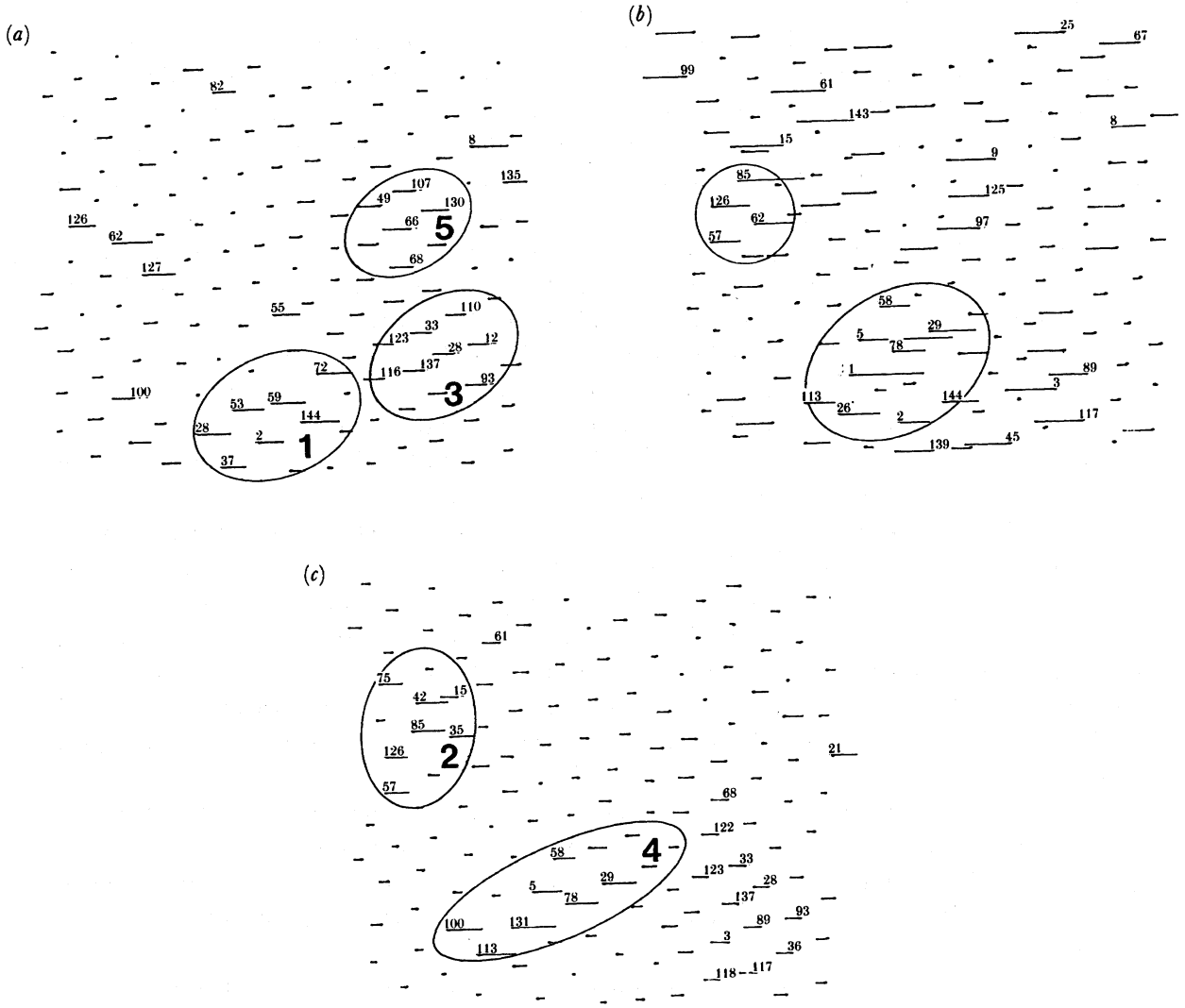

FIGURE 6. Field of excess properties averaged over the entire simulation period: (*a*) volume per atom; (*b*) enthalpy; (*c*) site distortion parameter.

distortion, atomic site pressure, maximum shear stress and atomic site modulus, as a function of time of simulation, were examined in detail. From this examination it was noted that cluster 1, which has the most extreme excesses in volume, showed the most dramatic relaxations in volume, in enthalpy, in site distortion, in rise in pressure and in rise in shear modulus, mostly by undergoing a decrease in dilatation. Clusters 3 and 5 with the minimum excesses in properties, showed no important changes, but exhibited only flutter. Clusters 2 and 4, which had large initial site distortions, showed larger variations in enthalpy, site distortion, pressure and shear stress, but no systematic changes.

4. Discussion

Isothermal structural relaxations in real amorphous media at about half the glass transition temperature would be comparatively very slow processes. In metallic glasses such as the Cu_xZr_{1-x} glasses that have been simulated here, structural relaxations have characteristic time constants that are closely comparable to those found in anelastic relaxations (Deng & Argon 1986*b*) and have activation energies that span between 1–2 eV and frequency factors that are in the range of 10^{10}–10^{12} s^{-1}. This gives ranges in relaxation time from 10–10^{13} s. Processes with such very long relaxation times cannot, of course, be simulated by MD. Therefore, in the simulation reported here, rather artificial initial conditions were taken, in which an alloy at its melting point was quenched at infinite rate to a low temperature, where it had an extremely large excess of properties that could be relaxed. The time span in the relaxation that could be reasonably simulated consisted of only 200 thermal fluctuations at a temperature equal to 0.556 of T_g, i.e. over a period differing from the required real times by 10–11 decades. Consequently, the results presented here cannot be compared directly with those of metallic glasses under any realistic conditions. Therefore, these results must be examined primarily for the qualitative information that they convey, for the chronological ordering of processes, and the time independent kinematics of structural relaxation. This is also apparent from the distribution function of activation energies for relaxation of excess enthalpy, volume per atom and distortion that were calculated by matching a Williams–Watts relaxation function to the results of the simulation. The distribution function has a peak at $\Delta G^*/E_0 = 0.45$. As the scaling factor $E_0 = 0.15$ eV for this simulation (see part I), the observed characteristic activation energy is 0.068 eV and not 1.5 eV, as is the case for the real Cu_xZr_{1-x} alloy. Clearly, the only processes that can be relaxed over such short periods of time are those that appear in the simulation. Indeed, if this activation energy and its associated relaxation period of seven fluctuations are taken as accurate, and a formal upward scaling of relaxation times to $\tau_2 = 4$ s (a 0.25 Hz internal friction experiment) at $T = 0.556\,T_g$ of a $Cu_{59}Zr_{41}$ glass having a T_g of 741 K is done, according to a direct scaling relation of $\Delta G_2^* = \Delta G_1^* + kT\ln(\tau_2/\tau_1)$, an activation energy of $\Delta G_2^* = 1.05$ eV is obtained, where $\Delta G_1^* = 0.068$ eV, $\tau_1 = 7 \times 5.4 \times 10^{-13}$ s and $T = 412$ K have been used from the simulation. This is almost exactly the lowest energy in the spectrum of energies measured in internal friction experiments (at 0.25 Hz) by Deng & Argon (1986*b*), which can produce relaxation at such a low homologous temperature. Thus when properly scaled up, the results of the simulation are consistent also with experimental results. This, however, implies a similarity in the shapes of energy spectra at the atomic fluctuation scale with energies in the macroscopic scale, for which no clear justification can be furnished.

Considering the results of the simulation as a whole, we have shown that structural

relaxations are complex and cooperative processes. The excess structural properties in the form of excess enthalpy, volume per atom (free volume), site distortion, atomic level stresses and moduli are not uniformly spread out in the structure. The excess enthalpy, free volume and site distortion show the greatest degree of clustering, while the atomic level stresses cluster less, because they are associated more directly with the Zr and Cu atoms, which were randomly distributed in the initial state of the structure. At the temperature of simulation ($0.556\,T_g$) the relaxation is to a large extent a local and immobile one, i.e. the clusters with large excess show a decay in their properties by local atom motions. There were no important displacements of regions with large free volume toward regions with deficiencies in free volume, i.e. so-called n-type clusters were not observed in any meaningful way to migrate to p-type clusters, as described by Egami & Vitek (1983) from their simulations. Although such 'interdiffusion' of defect clusters is very appealing, and may probably occur in more realistic situations in real time, they must require much longer periods of time, in excess of the simulation period studied here. We recall from part II that the topological features of the relaxation involve a reduction in the volume fraction of atom sites with five and seven near neighbours, i.e. reduction of liquid-like boundary material by gradual dismemberment and dissipation of such regions, as they are replaced by a growth of quasi-ordered material consisting of atoms with six near neighbours. In part IV we demonstrate that it is this liquid-like boundary material that seeds shear transformations, which are the principal modes of strain production in aged amorphous material before the ordered domains become large enough to permit plasticity by dislocation glide.

The research reported here has received support from a number of different sources. The principal one of those was an NSF Grant No. DMR-85-17224. Other support, particularly for computations, came in the early phases from the Center of Materials Science and Engineering at MIT from the basic NSF/MRL Grant DMR-84-18718, and in its final stages from the Defense Advanced Research Projects Agency under Contract N00014-86-K-0768. Additional salary support for D.D. was provided by the Allied Signal Corporation through a fellowship, for which we are grateful to Dr Lance Davis. S.Y. also acknowledges the support of NSF under grants CHE-84-15078 and CHE-88-06767.

Appendix 1. Boundary masses

To maintain the external pressure constant in MD simulations, Andersen (1980) introduced another dynamic coordinate into the basic lagrangian representing the equations of motion of the atoms in the simulation. The new coordinate Q representing the volume of the simulation cell then gives the modified lagrangian:

$$L(\rho_i, \dot{\rho}_i, Q, \dot{Q}) = \tfrac{1}{2}mQ^{\frac{2}{3}} \sum_{i=1}^{n} \dot{\rho}_i \cdot \dot{\rho}_i - \frac{1}{2} \sum_{\substack{j=1 \\ j \neq i}}^{n} \phi(Q^{\frac{1}{3}}\rho_{ij}) + \tfrac{1}{2}M\dot{Q}^2 - \alpha Q, \qquad \text{(A 1)}$$

where all quantities have been defined earlier in §2.2 of the text.

To minimize artifacts of unwanted resonances of the fictitious boundary masses and the atoms in the simulation cell, it is necessary to choose the boundary mass carefully, not to affect the kinetics of any process that is being simulated. The recommended procedure is to chose M in such a way that the period of the fluctuations of Q is approximately equal to $Q^{\frac{1}{3}}$ divided by

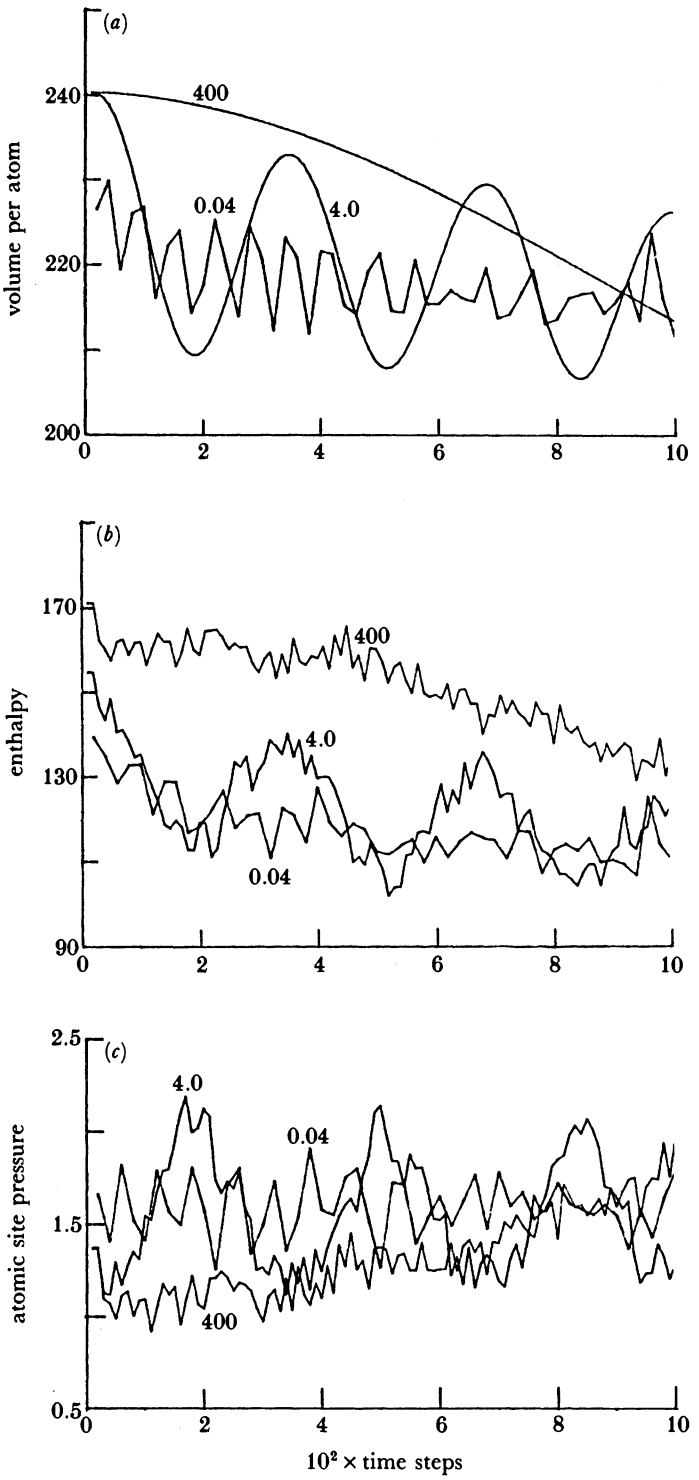

FIGURE 7. Effect of choice of boundary mass on the relaxation of excess properties: (*a*) volume per atom; (*b*) enthalpy; (*c*) atomic site pressure.

the speed of sound in the simulation cell. As discussed in §2.2, this criterion gave a boundary mass of 4 atom masses. Nevertheless, to explore the effect of the boundary mass on the results of the simulation, other values one hundredth of the chosen value and hundred times the chosen value were also used to determine the effect of the choice.

Figure 7*a–c* show the results of a relaxation simulation of the volume, enthalpy, and internal pressure for the three different boundary masses. Clearly, the responses to boundary masses of 0.04 and 400 give insufficient damping and erratic behaviour or supercritical damping respectively during the period of simulation lasting 1000 time steps (50 fluctuations). The results for the boundary mass of 4 show rather regular oscillations in properties that were presented already above. These could be readily isolated and discounted when necessary.

References

Andersen, H. C. 1980 *J. chem. Phys.* **72**, 2384.
Argon, A. S. 1968 *J. appl. Phys.* **39**, 4080.
Argon, A. S. & Kuo, H-Y. 1980 *J. non-cryst. Solids* **37**, 241.
Bendler, J. T. & Shlesinger, M. F. 1985 *Macromolecules* **18**, 591.
Deng, D. & Argon, A. S. 1986*a* *Acta metall.* **34**, 2011.
Deng, D. & Argon, A. S. 1986*b* *Acta metall.* **34**, 2025.
Deng, D., Argon, A. S. & Yip, S. 1989*a* *Phil. Trans. R. Soc. Lond.* A **329**, 549. (Part I of this issue.)
Deng, D., Argon, A. S. & Yip, S. 1989*b* *Phil. Trans. R. Soc. Lond.* A **329**, 575. (Part II of this issue.)
Deng, D., Argon, A. S. & Yip, S. 1989*c* *Phil. Trans. R. Soc. Lond.* A **329**, 613. (Part IV of this issue.)
Egami, T. & Vitek, V. 1983 In *Amorphous materials: modelling of structure and properties* (ed. V. Vitek), p. 127. New York: AIME.
Kobayashi, S., Maeda, K. & Takeuchi, S. 1980 *Acta metall.* **28**, 1641.
Kobayashi, S. & Takeuchi, S. 1984 *J. Phys.* F **14**, 23.
Kohlrausch, F. 1863 *Pogg. Ann. Physik* **119**, 352.
Lindsey, C. P. & Patterson, G. D. 1980 *J. chem. Phys.* **73**, 3348.
Maeda, K. & Takeuchi, S. 1982 *J. Phys.* F **12**, 2767.
Novick, A. S. & Berry, B. S. 1972 *Anelastic relaxation in crystalline solids.* New York: Academic Press.
Primak, W. 1955 *Phys. Rev.* **100**, 1677.
Schlesinger, M. F. & Montroll, E. W. 1984 *Proc. natn. Acad. Sci. U.S.A.* **81**, 1280.
Takeuchi, S., Maeda, K. & Kobayashi, S. 1983 In *Amorphous materials: modelling of structure and properties* (ed. V. Vitek), p. 305. New York: AIME.
Williams, G. & Watts, D. C. 1970 *Trans. Faraday Soc.* **66**, 80.

PHILOSOPHICAL TRANSACTIONS OF THE ROYAL SOCIETY A MATHEMATICAL, PHYSICAL & ENGINEERING SCIENCES